Taras Patsahan, ICMP, Lviv

During my stay in Lublin I prepared the manuscript of a new paper, concerning the behavior of linear and Y-shaped brushes in contact with solvents of differemt quality. This task was done in collaboration with T. Staszewski. I also discussed several problems with Prof. A. Patrykiejew. Moreover, I delivered a seminar "Structure of linear and Y-shaped polymer brushes in a solvent of different quality: molecular dynamics study" for the stuff and students of the Department for the Modelling of Physico-Chemical Processes, UMCS.

The sketch draft of the paper is enclosed below.

Structure of linear and Y-shaped polymer brushes in a solvent of different quality: molecular dynamics study

S. Sokołowski, T. Staszewski

Department for the Modelling of Physico-Chemical Processes,

Maria Curie-Skłodowska University, 20031 Lublin, Poland

T. Patsahan

Institute for Condensed Matter Physics of the National Academy of Sciences of Ukraine,

1 Svientsitskii Str., 79011 Lviv, Ukraine

Abstract

Linear and Y-shaped polymer brushes in a solvent of different quality are studied using the method of molecular dynamics. The density profiles of polymer and solvent species at different conditions are obtained and analyzed. It is seen that increasing of attraction between polymers and solvent causes layering effects and changes in a brush thickness. Also we calculated such quantities as a gyration radius and an end-to-end distance of brush polymers. A non-monotonous behavior of the temperature dependencies for the given characteristics is observed when a solvent is poor. On the other hand a stretching of polymers leads to monotonous increasing of the considered quantities in a good solvent. From snapshots of simulated systems a qualitative difference in a brush structure depending on a quality of solvent is noticed. For instance the polymers can form clusters in a poor solvent, and at high temperatures these clusters disappear while a homogeneous polymer brush is obtained. In a good solvent these clusters are not observed at all.

I. INTRODUCTION

In our investigation we considered the systems of a solvent confined in a slit-like pore with a wall modified by tethered linear and Y-shaped polymers forming a brush. We are aimed to study distributions of polymer particles composing the brush as well as a solvent density profiles in the pore at different conditions: temperature, amount of a solvent, interaction between solvent and polymer particles. Therefore, a series of molecular dynamics simulations are performed and the corresponding structural characteristics for polymer and solvent species are obtained and analyzed.

II. MODELS AND SIMULATION DETAILS

The simulated systems consist of a polymer brush in a solvent confined between two parallel flat walls. The polymer brush is grafted to one of the walls. Schematically this system is presented in Fig. 1. The grafting particles of polymers are placed randomly at the distance to the wall $\Delta z = 0.01$ and their positions are fixed. The interactions of solvent and polymer particles with the walls are of a hard-core type, while for the description of an interaction between particles the Lennard-Jones potential is used:

$$U_{\alpha\beta} = 4\varepsilon_{\alpha\beta}\left[\left(\frac{\sigma_{\alpha\beta}}{r}\right)^{12} - \left(\frac{\sigma_{\alpha\beta}}{r}\right)^{12}\right], \tag{1}$$

where on places of the indices α and β the polymer (p) and the solvent s species are implied. The bonds in polymers are described by the finitely extensible nonlinear elastic (FENE) potential:

$$U_{\mathrm{FENE}}(r) = -0.5KR_0^2 \ln\left[1 - \left(\frac{r}{R_0}\right)^2\right] + 4\varepsilon_{pp}\left[\left(\frac{\sigma_{pp}}{r}\right)^{12} - \left(\frac{\sigma_{pp}}{r}\right)^{12}\right] + \varepsilon_{pp}. \tag{2}$$

The distance between the walls is set large enough to get a bulk-like region of the solvent in a middle region of the pore and equal to $L_z = 40.0$. The sizes of particles are taken the same both for the polymer and solvent species, $\sigma_{\alpha\beta} = 1.0$. The total number density of solvent particles in the system, $\rho = N/V$, is considered in the range $0.4 - 0.7$. In our study the parameters of Lennard-Jones (LJ) potential for the polymer, ε_{pp}, and the solvent, ε_{ss}, are set equivalent $\varepsilon_{pp} = \varepsilon_{ss} = 1.0$, while the polymer-solvent LJ parameter ε_{ps} varies in the wide range $\varepsilon_{ps} = 1.0 - 5.0$. The parameters of FENE potential (2) are chosen as $K = 50.0$

and $R_0 = 1.3\sigma$. All the interactions in the studies systems are cut off at the distance $r_{cut} = 3.0$. All the quantities in the given study are presented in the reduced LJ units. Two architectures of polymers are considered in our study: linear and Y-shaped molecules. To distinguish an effect of the polymer structures we fix a total density of polymer particles as well a geometrical length of the polymer molecules. The linear polymers consist of $N_L = 18$ monomers and the grafting density is set to $\sigma_g = 0.1$. A size of simulation box in XY-plane is set $L_x = L_y = 32.0$, thus a number of polymer chains in the simulated system is 102. Hence, the surface density of polymer particles is equal to $\rho_p = N_L\sigma_g = 1.8$. The Y-shaped polymer is built by attaching a side chain of length 8 to the 10-th particle of the linear polymer (Fig. 2). Therefore, one obtains a symmetrical Y-shaped molecule of the same length as the linear molecule, i.e. the maximum end-to-end distance of Y-shaped molecule is 18. However, a number of particles composing this molecule is higher than in the case of linear molecule, $N_Y = 26$. If one fixes polymer particles density at $\rho_p = 1.8$, than the grafting density for the Y-shaped polymers should be adjusted as $\sigma_g' = \rho_p/N_Y \simeq 0.069$. For the Y-shaped brush a larger simulation box is used, $L_x = L_y = 40.0$, although a distance between the walls is remained the same as for the linear polymer brush ($L_z = 40$). Therefore, the corresponding number of Y-shaped molecules is 110.

The described models are simulated using the method of molecular dynamics. The simulations were performed in three stages. First stage is a preliminary equilibration of a system at a low temperature ($T = 1.0$) using simple rescalling of particle velocities. The second one is the equilibration in the NVT ensemble at the required temperature ($T = 1.0 - 2.6$) with the Nose-Hoover thermostat applied. The third stage is used for a production of results and it is performed in the NVE ensemble. During this stage we calculated polymer and solvent density profiles $\rho_p(z)$ and $\rho_s(z)$, the first and second momenta of the density profiles for polymer brush $< z >$ (brush thickness) and $< z^2 >$, a radius of gyration R_g and an end-to-end distance R_{1N} of polymer chains. From the momenta $< z >$ and $< z^2 >$ the root mean-square roughness (RMS) of polymer brush layer is obtained. Also we estimated a longest axis of an ellipsoid a, which effectively describes a polymer chain. We have checked a system at different temperatures in the range $T = 1.0 - 2.6$.

$$\langle z \rangle = \frac{1}{\rho L_z} \int_0^{L_z} z \rho_p(z) dz \tag{3}$$

$$\left\langle z^2 \right\rangle = \frac{1}{\rho L_z} \int_0^{L_z} z^2 \rho_p(z) dz \tag{4}$$

$$R_q = \sqrt{\left\langle z^2 \right\rangle - \left\langle z \right\rangle^2} \tag{5}$$

III. RESULTS AND DISCUSSION

A. Linear polymer brush

The density profiles for the linear polymer brush ($\rho_s(z)$) and the solvent ($\rho_s(z)$) are obtained for the different values of energy parameter ε_{ps} as well as for the different temperatures T (Figs. 3-6). In figures (Figs. 3a-6a) one can observe three distinct maxima of $\rho_p(z)$ for $\varepsilon_{ps} = 1.0$ and temperature $T = 1.0$ (red line). Increasing of temperature leads to vanishing of the third maximum and the profile becomes smoother. At high densities (Fig. 6a) there is a tendency of the fourth maxima formation, which is rather small in a comparison with those three. However, the fourth maximum becomes essential when the attraction between solvent and polymer species is stronger ($\varepsilon_{ps} \geq 1.5$). In Figs. 3b-6b one can see already four maxima, two of which are vanishing with temperature increasing. An increase of ε_{ps} (up to $\varepsilon_{ps} = 5.0$) leads to the larger number of maxima on the density profiles of $\rho_p(z)$ at the fixed temperature $T = 1.4$ (Figs. 3c-6c). Simultaneously, the layering of solvent particles as well as their local density increase near the wall are observed. However, from the figures is seen that the temperature causes an opposite effect on a solvent – a lesser amount of fluid is located in the brush layer at higher temperatures. Nevertheless, the contact value of solvent with the wall increases in this case. It is worth mentioning that the bulk density of solvent in all considered cases is not necessarily equal to the density ρ, which is set as the total density of solvent particles in the system and it is clearly seen in the figures. In Table I we present correspondences between the parameter ρ and the bulk solvent density, which are obtained obtained from the plateaus in the solvent density profiles $\rho_s(z)$ at $z \approx 16.0$. It should be noted that sometimes a plateau cannot be found due to the strong phase separation. For instance, at the solvent density $\rho = 0.4$, the temperature $T = 1.0$ and $\varepsilon_{ps} = 1.5$ a condensation of the solvent at the brush and pure liquid phase in the opposite side of the box are observed, and these two phases are separated by the gas phase. Therefore, no plateau liquid bulk phase is formed in this case. In all other considered cases bulk-like phases are

present, but their densities can vary depending on the set conditions. Also from the figures is seen that a width of the polymer brush density profile increases if the temperature increases or/and ε_{ps} increases, which can be explained by polymer stretching. The structural properties of the polymers are discussed below. Except the mentioned solvent condensation at the low density $\rho = 0.4$, no qualitative difference in the density profiles depending on the total density ρ is observed.

The temperature dependencies of the gyration radius R_g, the RMS roughness R_q, the largest axis of effective ellipsoid a and the brush thickness $< z >$ are presented in Fig. 7. We start this plots from $T = 1.4$, since phase instabilities appearing at the lower temperatures worsen statistics of our results in this region. One can see that these dependencies are non-monotonous and have a distinct minimum around $T = 2.0 - 2.0$ in the case of $\varepsilon_{ps} = 1.0$. We relate this minimum with a transition from polymers clusters (pinned micelles) to a homogenous (swallen) brush [1]. In Fig. 8 we present a snapshot with an illustration of polymers clustering observed at the temperature $T = 1.4$ when $\varepsilon_{ps} = 1.0$. A polymer brush after a clusters collapse is shown in Fig. 9. This snapshot is obtained at the temperature $T = 2.2$ and even at this temperature the polymers are not stretched well forming so called 'mashrooms'. If one takes higher value of ε_{ps}, i.e. equal to 1.5, all characteristics become larger than for $\varepsilon_{ps} = 1.0$ and they have a tendency for monotonous growing, which should obviously finish with a saturation at higher temperatures. On the other hand, a slow decrease is observed for the thickness $< z >$. Monotonous behaviour of the calculated dependencies at $\varepsilon_{ps} = 1.5$ can be explained by the fact that there is no clustering or 'pinned micelles' in this case, even at the temperature $T = 1.0$. In Fig. 10 one can see a homogeneous brush with the well stretched polymers.

Increasing of ε_{ps} leads to a stronger stretching of polymer molecules Fig. 11. Quantitatively, it is seen in Fig. 12, where the dependencies of R_g, R_q, a and $< z >$ on the interaction parameter ε_{ps} are shown. One can observe that an increase of ε_{ps} leads to the dramatic growth of the R_g, R_q, a, $< z >$. All presented characteristics have the same behavior, which exhibits a fast growth starting from $\varepsilon_{ps} = 1.0$ and finishing around $\varepsilon_{ps} = 3.5$. However, further increasing of ε_{ps} leads to a small lowering of the considered quantities.

B. Y-shaped polymer brush

In general a form of the density profiles of Y-shaped polymer brush and solvent particles looks similar to those for the case of linear polymer brush (Figs. 13-16). Qualitatively, except the strong separation at $\rho = 0.4$ and $\varepsilon_{ps} = 1.5$, everything observed for the linear polymer brush is noticed for Y-shaped polymer brush as well. However, some quantitative differences are found. For instance, the brush density profile of Y-shaped polymers is smoother than one of linear polymers. Therefore, all peaks at $\rho_p(z)$ are less distinguished and vanish faster if the temperature increases. The distribution of Y-shaped polymers is more skewed in the direction larger z, what is obvious, since a center of mass of these polymers usually should be located at the larger distance to the wall than of linear polymers. For the solvent density profiles one can see practically the same picture as for the case of linear polymer brush. However, in Fig. 16c there is somewhat different in comparison with other density profiles, e.g. the solvent density profile has more oscillations, but with less amplitude.

The effect of ρ is also not different as in the previous case. In Table II we present correspondence between ρ and the solvent bulk density. Anomalous behaviour is noticed only for the highest density $\rho = 0.7$ – a width of the brush layer keeps growing with ε_{ps} increasing for $\varepsilon_{ps} > 3.0$, and does stop not even at $\varepsilon_{ps} = 5.0$. This the only case when a such behaviour is obtained.

As previously, we present the temperature dependencies of the radius of gyration (R_g), the RMS roughness (R_q), the largest axis of effective ellipsoid (a) and the brush thickness ($< z >$) in figure Fig. 17. Qualitatively these results are not different to those obtained for the linear polymer brush. If $\varepsilon_{ps} = 1.0$ all considered characteristics are non-monotonous. They have a minimum around the temperature $T = 2.0 - 2.2$ which related to the transition of clusters collapse, which was observed for the linear polymer brush at the same conditions. For $\varepsilon_{ps} = 1.5$ (and higher) this transition does not exist, at least at temperatures $T \geq 1$. Therefore, the different behaviour for the characteristics R_g, R_q, a and $< z >$ is noticed: they are all monotonously growing, except the thickness $< z >$, which is lowering with increasing of temperature.

The dependence on the parameter interaction between solvent particles and polymer particles, ε_{ps}, also shows a similar behaviour to that observed for the linear polymer brush. In Fig. 18 one can see an increase of R_g, R_q, a and $< z >$ up to $\varepsilon_{ps} = 2.5 - 3.0$ and then

they decreases. However, at the density $\rho = 0.7$ they continue to grow even at $\varepsilon_{ps} = 5.0$. Obviously, this effect is related somehow with the anomaly noticed in the density profiles mentioned above. Below, we will try to understand an origin of this strange behaviour by analyzing the end-to-end distance for linear and Y-shaped polymers.

In Figs. 19 and 20 we present the average end-to-end distances of the linear polymers R_{1N} depending on temperature and ε_{ps}, respectively. As is seen they qualitatively repeat R_g, R_q and a. Since, the Y-shaped polymer has three ends, thus three end-to-end distances can be measured. It is impossible to make a direct comparison of the R_{1N} obtained for the linear polymers with the end-to-end distances of Y-shaped polymers. Moreover, the question how to define the end-to-end distances Y-shaped polymer itself, at least two (free) ends are statistically undistinguished. In this case we suggest to consider a distribution of end-to-end distance between grafting particle and two other terminating particles on the arms of the Y-shaped molecule...

IV. CONCLUSIONS

---

[1] S. Minko, Polym. Rev., 2006, 46, 397.

TABLE I: Bulk densities at different total densities of a fluid. Case of the linear polymer brush.

ρ	T	ε_{ps}			
		1.0	1.5	3.0	5.0
0.4	1.0	0.63	-	-	-
	1.4	0.40	-	0.34	0.33
	1.8	0.40	0.39	-	-
	2.6	0.40	0.40	-	-
0.5	1.0	0.63	0.63	-	-
	1.4	0.51	-	0.46	0.45
	1.8	0.5	0.5	-	-
	2.6	0.5	0.5	-	-
0.6	1.0	0.65	0.64	-	-
	1.4	0.61	-	0.57	0.56
	1.8	0.61	0.60	-	-
	2.6	0.61	0.60	-	-
0.7	1.0	0.71	0.70	-	-
	1.4	0.71	-	0.68	0.67
	1.8	0.71	0.70	-	-
	2.6	0.71	0.70	-	-

TABLE II: Bulk densities at different total densities of a fluid. Case of the Y-shaped polymer brush.

ρ	T	ε_{ps}			
		1.0	1.5	3.0	5.0
0.4	1.0	0.63	0.63	-	-
	1.4	0.41	-	0.34	0.32
	1.8	0.40	0.63	-	-
	2.6	0.40	0.40	-	-
0.5	1.0	0.63	0.63	-	-
	1.4	0.51	-	0.46	0.44
	1.8	0.50	0.49	-	-
	2.6	0.50	0.49	-	-
0.6	1.0	0.64	0.64	-	-
	1.4	0.61	-	0.57	0.55
	1.8	0.61	0.60	-	-
	2.6	0.61	0.60	-	-
0.7	1.0	0.71	0.70	-	-
	1.4	0.71	-	0.68	0.67
	1.8	0.71	0.70	-	-
	2.6	0.71	0.70	-	-

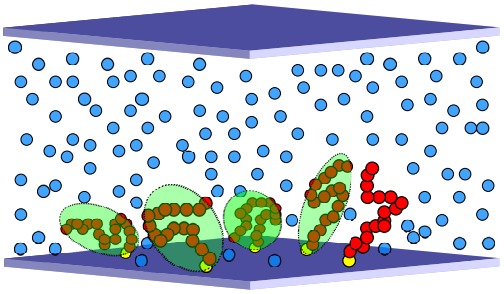

FIG. 1: Schematic presentation of the model under study. Two parallel planes describe two walls of the pore. Red circles denote polymer particles. Yellow circles are grafting particles. Blue circles denote solvent particles. Green ellipses surrounding polymer chains denote effective ellipsoids.

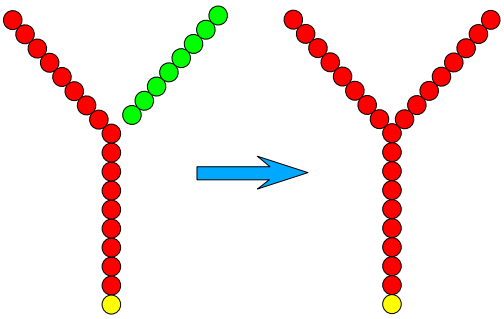

FIG. 2: An Y-shaped molecule (to the right) constructed by attaching of a side chain (green circles) to the linear polymer molecule (to the left). Yellow circles are grafting particles.

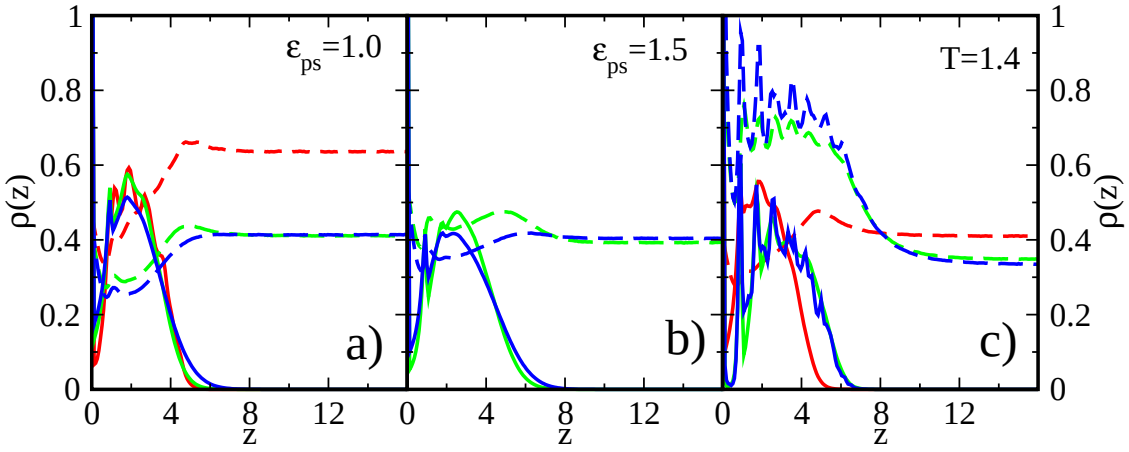

FIG. 3: Density profiles of the linear polymer and solvent species at the density $\rho = 0.4$: (a) $T = 1.0$ (red), $T = 1.8$ (green), $T = 2.6$ (blue); (b) $T = 1.8$ (green), $T = 2.6$ (blue); (c) $\varepsilon_{ps} = 1.0$ (red), $\varepsilon_{ps} = 3.0$ (green), $\varepsilon_{ps} = 5.0$ (blue).

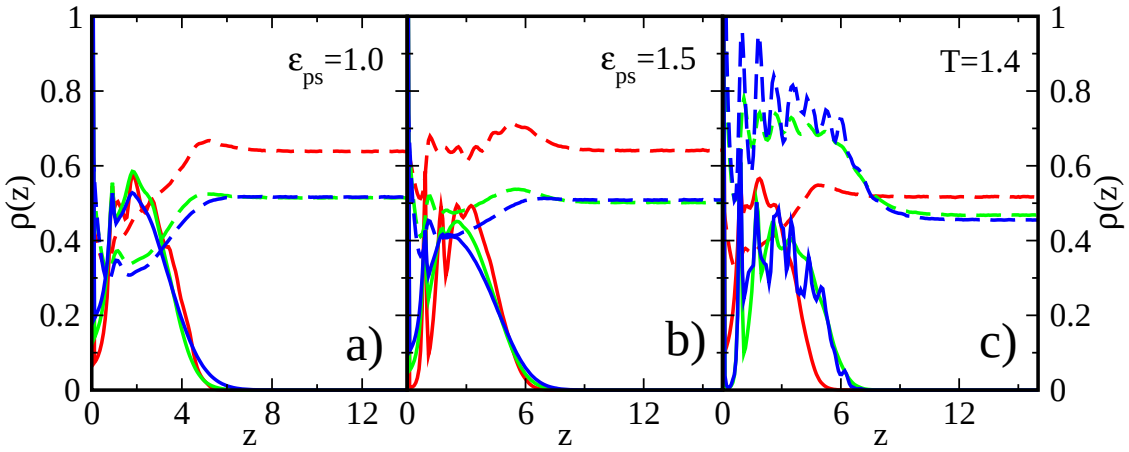

FIG. 4: Density profiles of the linear polymer and solvent species at the density $\rho = 0.5$: (a) $T = 1.0$ (red), $T = 1.8$ (green), $T = 2.6$ (blue); (b) $T = 1.0$ (red), $T = 1.8$ (green), $T = 2.6$ (blue); (c) $\varepsilon_{ps} = 1.0$ (red), $\varepsilon_{ps} = 3.0$ (green), $\varepsilon_{ps} = 5.0$ (blue).

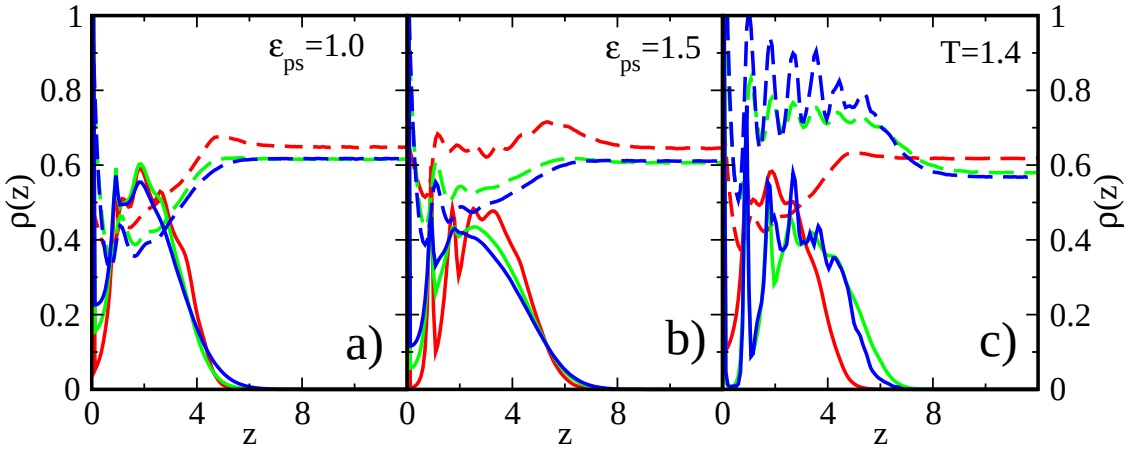

FIG. 5: The same as in Fig. 4, but at the solvent density $\rho = 0.6$.

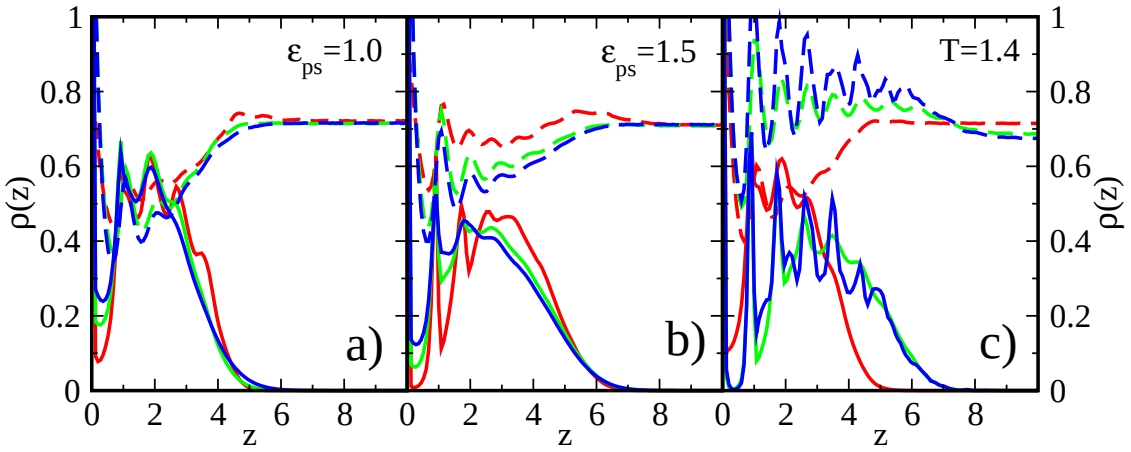

FIG. 6: The same as in Fig. 4, but at the solvent density $\rho = 0.7$.

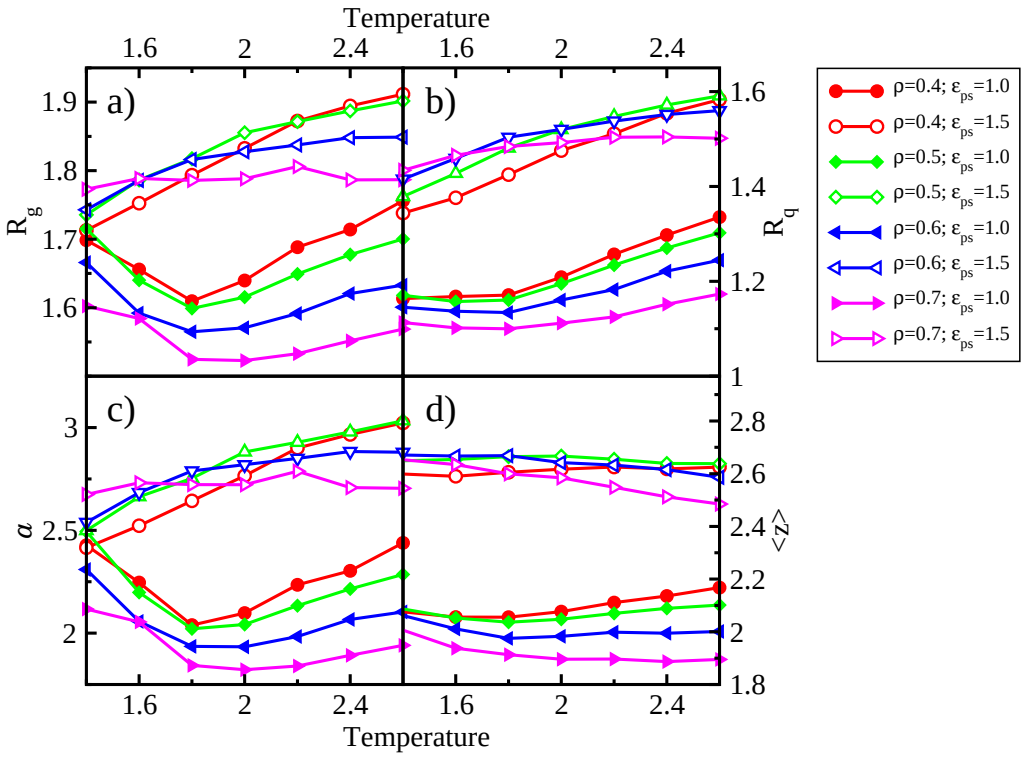

FIG. 7: The structure properties of the linear polymer at the different densities and the parameter ε_{ps}: (a) average of gyration radius of the polymer chains R_g; (b) RMS roughness of the polymer brush R_q; (c) average of the largest axis of an effective ellipsoid presenting the polymer chains a; (d) average thickness of the polymer brush $< z >$.

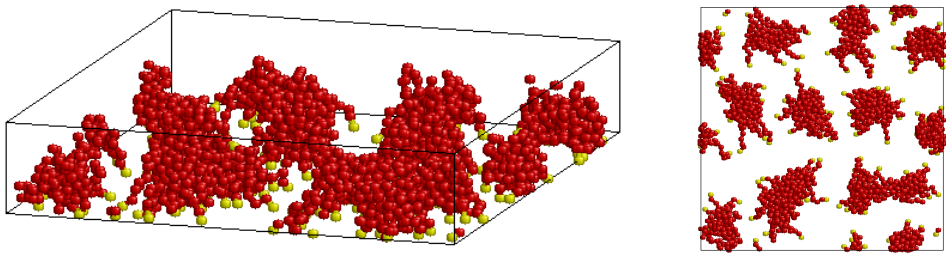

FIG. 8: Snapshot of the system with parameters $\rho = 0.6$, $\varepsilon_{ps} = 1.0$ and $T = 1.4$.

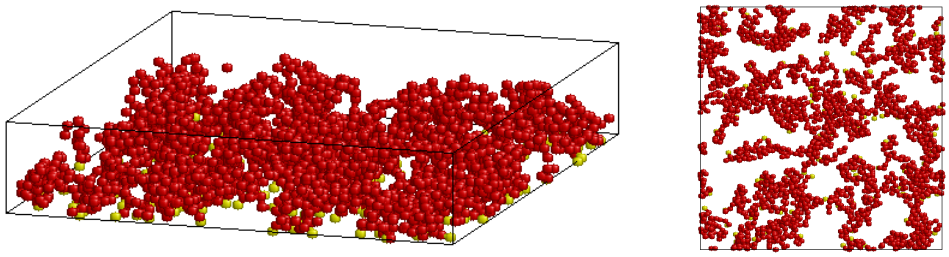

FIG. 9: Snapshot of the system with parameters $\rho = 0.6$, $\varepsilon_{ps} = 1.0$ and $T = 2.2$.

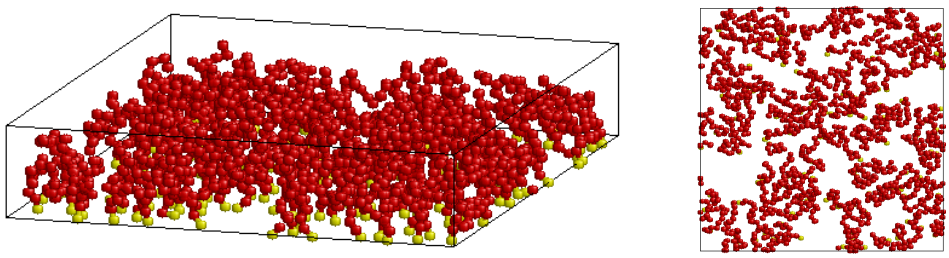

FIG. 10: Snapshot of the system with parameters $\rho = 0.6$, $\varepsilon_{ps} = 1.5$ and $T = 1.0$.

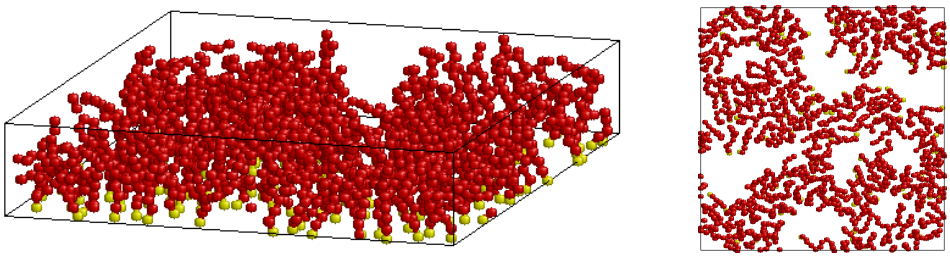

FIG. 11: Snapshot of the system with parameters $\rho = 0.6$, $\varepsilon_{ps} = 4.0$ and $T = 1.4$.

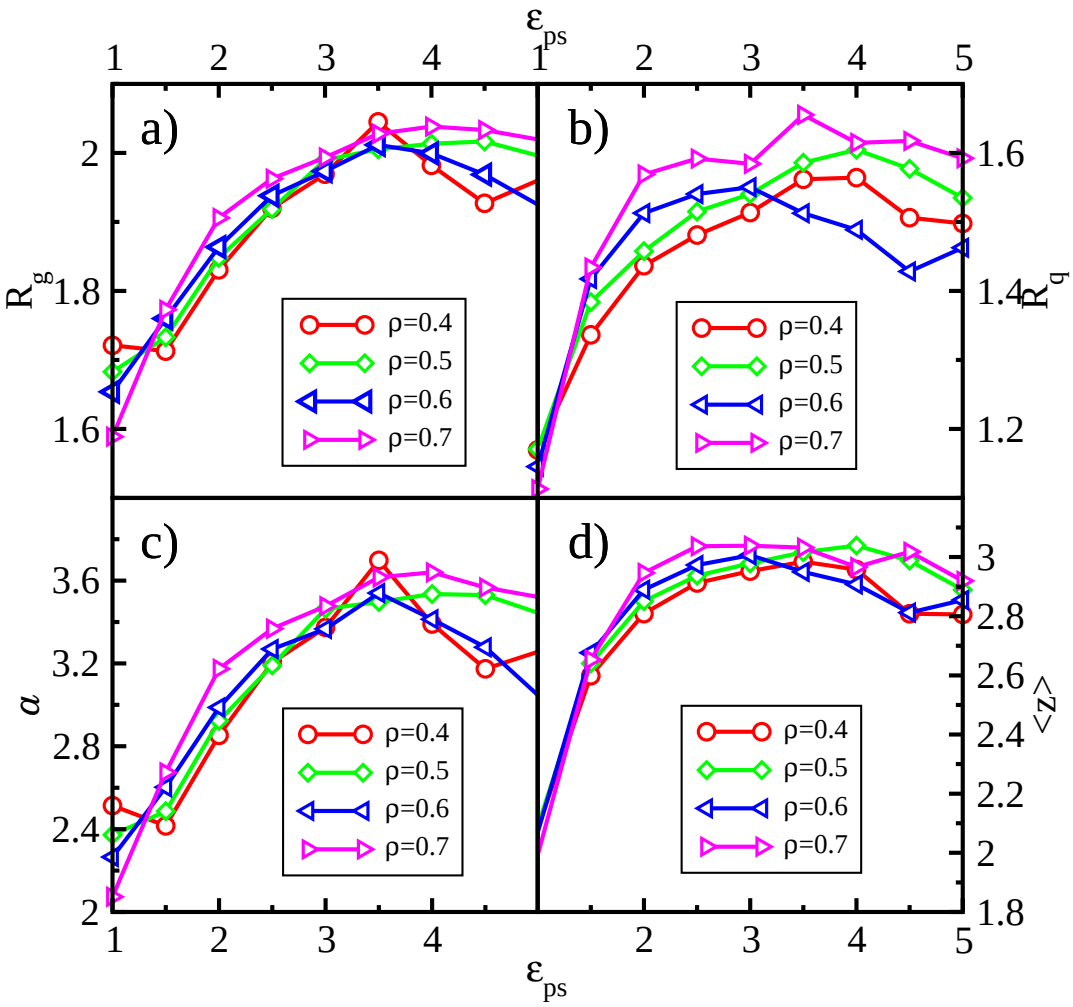

FIG. 12: The structure properties of the linear polymer at the different densities and the parameter ε_{ps}, but at the fixed temperature $T = 1.4$: (a) average of gyration radius of the polymer chains R_g; (b) RMS roughness of the polymer brush R_q; (c) average of the largest axis of an effective ellipsoid presenting the polymer chains a; (d) average thickness of the polymer brush $< z >$.

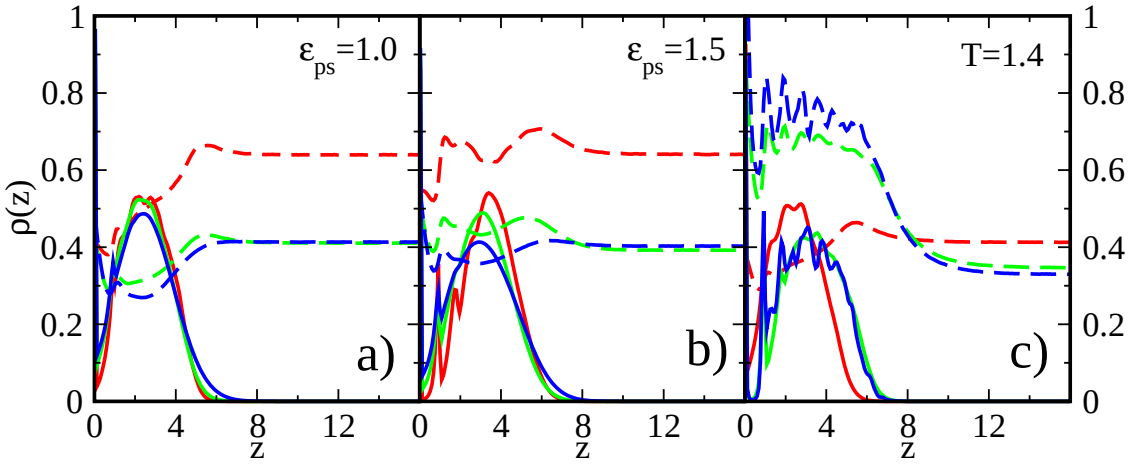

FIG. 13: Density profiles of the Y-shaped polymer and solvent species at the density $\rho = 0.4$: (a) $T = 1.0$ (red), $T = 1.8$ (green), $T = 2.6$ (blue); (b) $T = 1.0$ (red), $T = 1.8$ (green), $T = 2.6$ (blue); (c) $\varepsilon_{ps} = 1.0$ (red), $\varepsilon_{ps} = 3.0$ (green), $\varepsilon_{ps} = 5.0$ (blue).

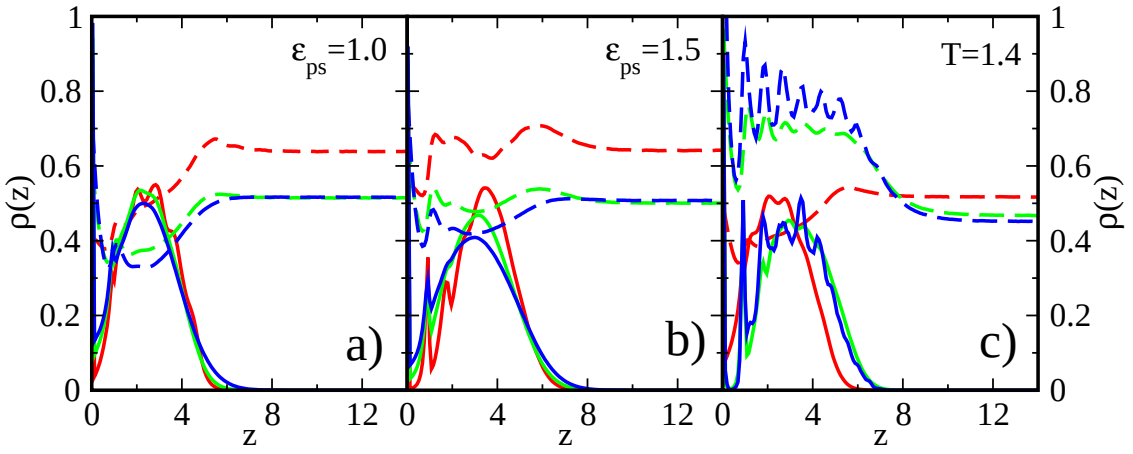

FIG. 14: The same as in Fig. 13, but at the solvent density $\rho = 0.5$.

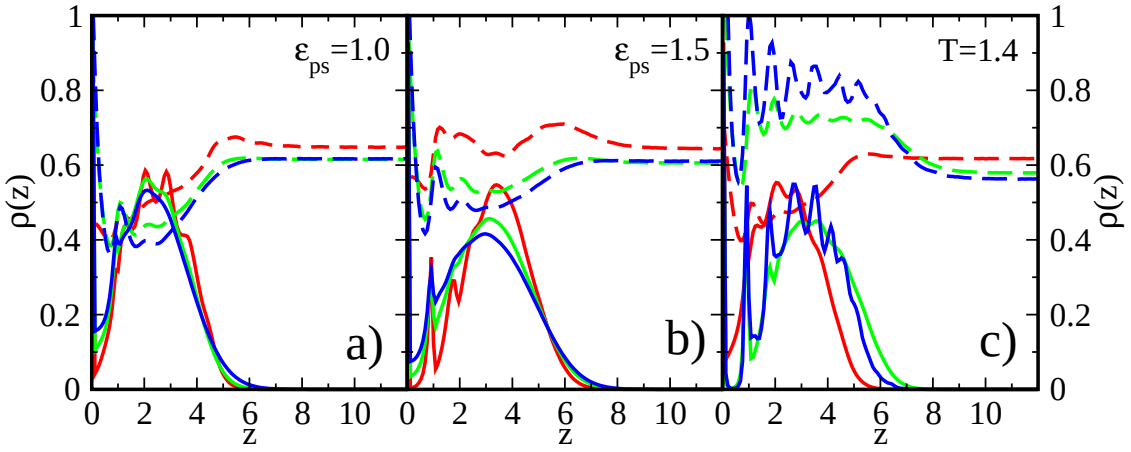

FIG. 15: The same as in Fig. 13, but at the solvent density $\rho = 0.6$.

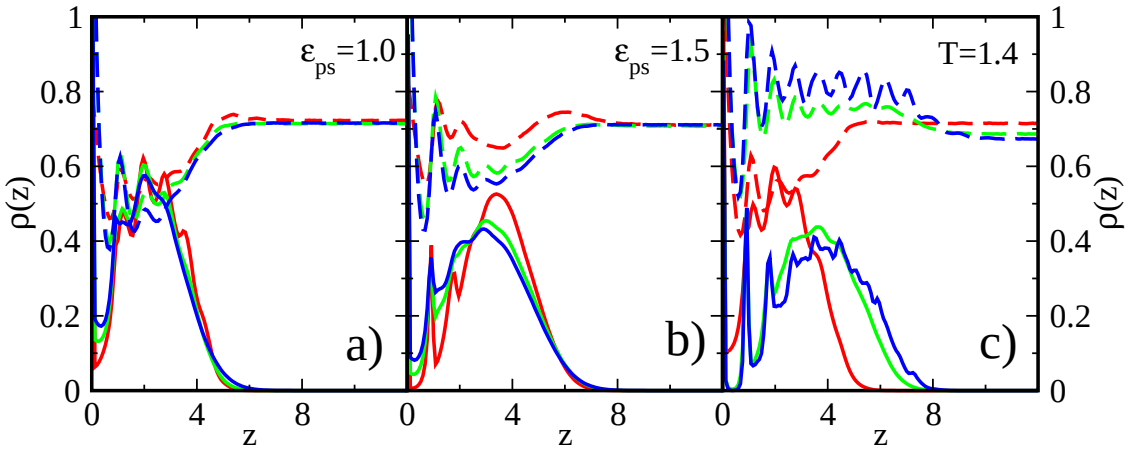

FIG. 16: The same as in Fig. 13, but at the solvent density $\rho = 0.7$.

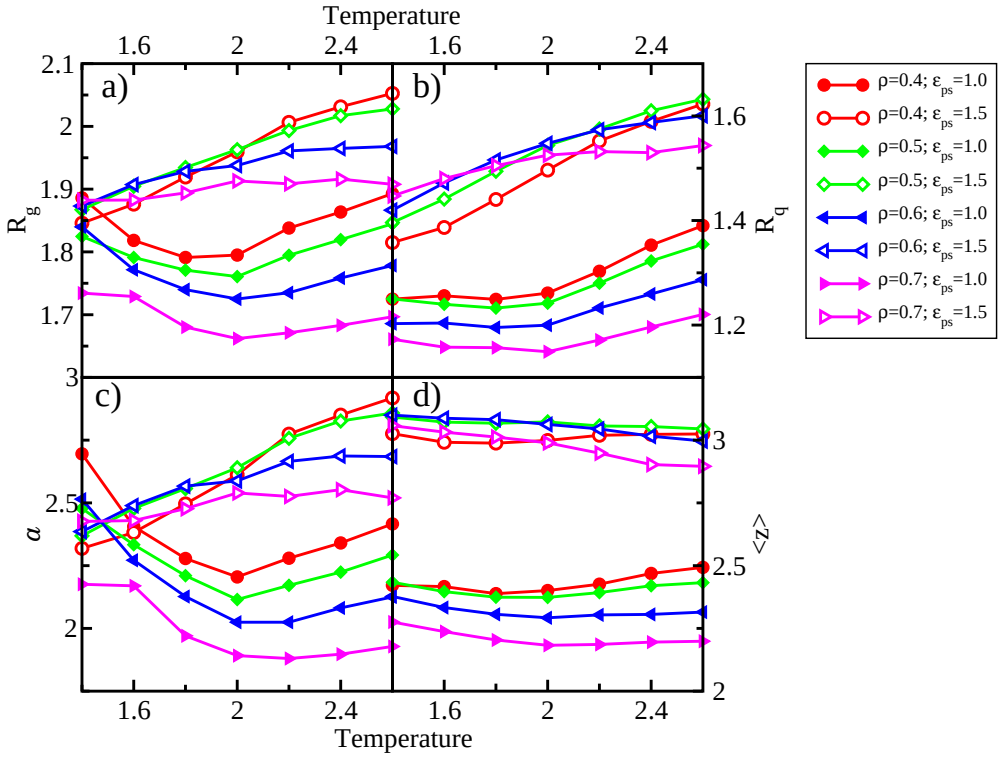

FIG. 17: The structure properties of the Y-shaped polymer at the different densities and the parameter ε_{ps}: (a) average of gyration radius of the polymer chains R_g; (b) RMS roughness of the polymer brush R_q; (c) average of the largest axis of an effective ellipsoid presenting the polymer chains a; (d) average thickness of the polymer brush $< z >$.

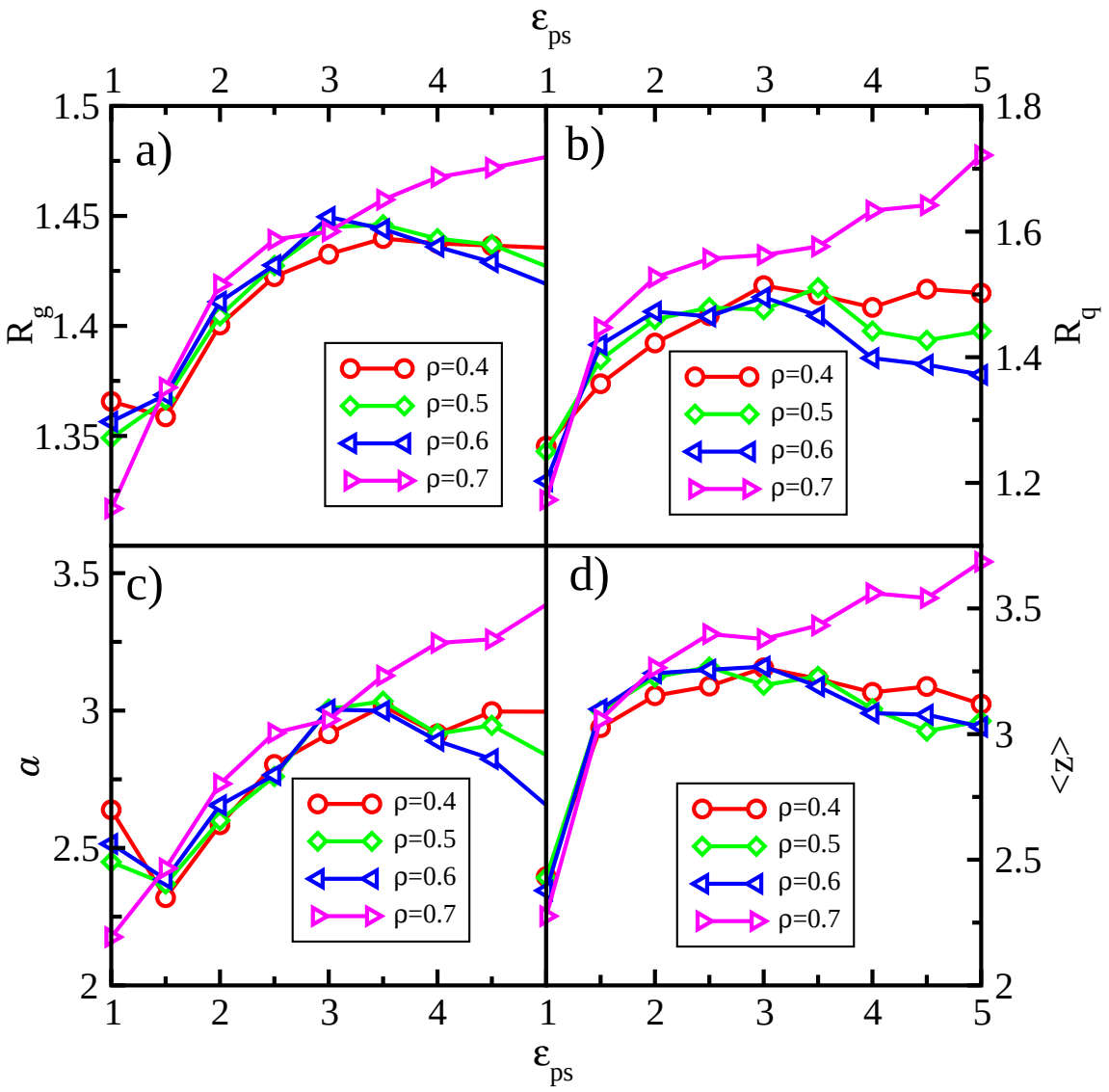

FIG. 18: The structure properties of the Y-shaped polymer at the different densities and the parameter ε_{ps}, but at the fixed temperature $T = 1.4$: (a) average of gyration radius of the polymer chains R_g; (b) RMS roughness of the polymer brush R_q; (c) average of the largest axis of an effective ellipsoid presenting the polymer chains a; (d) average thickness of the polymer brush $< z >$.

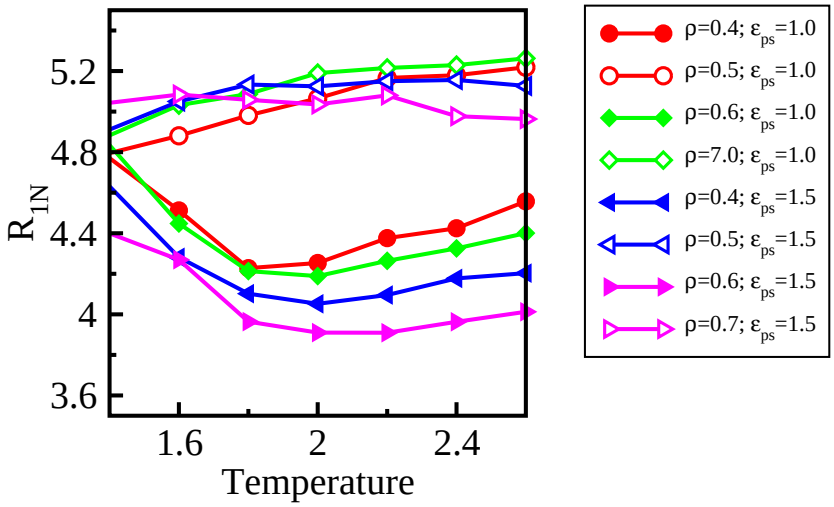

FIG. 19: Average end-to-end distance R_{1N} of the linear polymers at the different densities and the temperature, but at the fixed ε_{ps}.

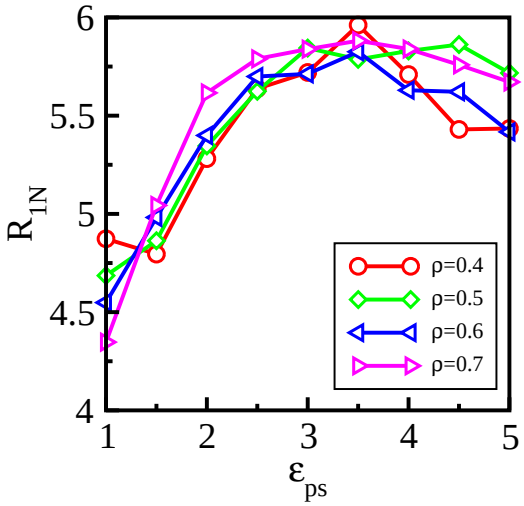

FIG. 20: Average end-to-end distance R_{1N} of the linear polymers at the different densities and the parameter ε_{ps}, but at the fixed temperature $T = 1.4$.